

DISKS AROUND CLASSICAL T TAURI STARS

P. D'Alessio,

Centro de Radioastronomía y Astrofísica, UNAM, Morelia, México

RESUMEN

En este trabajo explicamos como se pueden cuantificar las propiedades de los discos circunestelares y el polvo en estos, a partir de la comparación de observaciones y las propiedades observables de modelos físicos de discos irradiados por su estrella central. En particular se discuten las indicaciones de una evolución de la población de polvo de los discos alrededor de estrellas T Tauri.

ABSTRACT

We explain how observable properties of physically motivated models of accretion disks irradiated by their central stars can be compared with observations to quantify disk and dust properties. In particular, we discuss hints of dust evolution in disks around Classical T Tauri Stars.

Key Words: **ACCRETION : ACCRETION DISKS — STARS : PRE-MAIN SEQUENCE**

1. GENERAL

It is accepted that a large fraction of young stars are surrounded by dusty disks. They have been imaged in radio-frequencies with interferometers such as IRAM, VLA, BIMA, OVRO (see Dutrey et al. 1996; Wilner & Lay 2000) and at near-IR wavelengths using *HST* (see McCaughrean, Stapelfeldt & Close 2000; Krist et al. 2000) and adaptive optics (e.g. Koresko 1998; Jayawardhana et al. 2002). Although the possibility of imaging disks at subarc-second resolution is fairly recent, physical models of disks are twenty years old. These models explain spatially unresolved measurements, such as Spectral Energy Distributions (SEDs) and spectral lines of Classical T Tauri Stars (CTTS), Fu Ori stars, Ae/Be stars, etc. (e.g., Lynden-Bell & Pringle 1974; Kenyon & Hartmann 1987, 1995; Bertout, Basri & Bouvier 1987; Calvet et al. 1991, 1992; Malbet & Bertout 1992 and others).

According to the present standard view, a molecular core with non-zero angular momentum collapses, forming a star surrounded by a disk (e.g. Shu, Adams & Lizano 1997). The disk evolves, transferring angular momentum to a fraction of its material that moves towards larger distances, allowing the accretion of most of the disk mass onto the central star. The disk structure and evolution depends on the mechanism responsible for the angular momentum transfer (see Hartmann et al. 1998; Stepinski 1998), being the magneto-rotational instability the most accepted possibility to date (Balbus & Hawley 1991). There are several MHD simulations of a

disk patch, trying to quantify the viscosity coefficient produced by this and other mechanisms (see Stone et al. 2000). However, models of the whole disk structure and emission, frequently use the phenomenological α -prescription (Shakura & Sunyaev 1973), where a quantity α parametrizes the viscosity coefficient (e.g., Bell & Lin 1994; D'Alessio et al. 1998; 1999).

Closer to the star, the stellar magnetic field channel disk material into a magnetospheric flow that ends at an accretion shock on the stellar surface (see Muzerolle, Calvet & Hartmann 2001, and references therein). Spectroscopic and photometric variability support this idea of this magnetically controlled accretion (Bertout et al. 1988; Alencar, Johns-Krull & Basri 2001), and measured stellar magnetic fields of several kG are consistent with the requirements of the theory of magnetospheric accretion (Johns-Krull, Valenti & Koresko 1999; Johns-Krull & Valenti 2000). Furthermore, models of the accretion shock formed at the stellar surface (Calvet & Gullbring 1998; Ardila & Basri 2000; Gullbring et al. 2000) can explain the blue/UV excess observed in all CTTS, and models of the line profiles formed in the magnetospheric flow have successfully reproduced observations (Hartmann, Hewitt & Calvet 1994; Muzerolle, Hartmann & Calvet 1998a).

From a detailed analysis of veiling in the U band, Gullbring et al. (1998) find that CTTS are accreting material from their disks with rates between 10^{-9} and $10^{-7} M_{\odot} \text{ yr}^{-1}$, with a typical value around $\dot{M} = 10^{-8} M_{\odot} \text{ yr}^{-1}$. For such low \dot{M} , the accretion luminosity is often lower or similar to the stellar luminosity. The stellar irradiation flux onto a flat

disk has similar radial distribution and order of magnitude as the flux produced by viscous dissipation. However, Kenyon & Hartmann (1987) realized that under the effects of the stellar gravity and its own thermal pressure, the disk scale height increases with radius. As long as some dust is suspended along with the gas, the disk surface would efficiently absorb a larger fraction of stellar radiation than a flat disk. In particular, the stellar radiation is characterized by a shorter wavelength than the disk own thermal radiation field and it propagates inside the disk in a slanted direction, being mostly deposited in the upper layers of the disk atmosphere. This produces a temperature inversion (Calvet et al. 1991, 1992; Malbet & Bertout 1991; Chiang & Goldreich 1997; D’Alessio et al. 1998). Radiation scattered and reprocessed by this upper thin layer penetrates deeper, heating the disk photosphere from where most of the continuum radiation emerges. Thus, most of the infrared emission from disks is reprocessed stellar radiation. Only close to the midplane and at small radii, viscous dissipation becomes an important heating source.

The present contribution summarizes the work described by D’Alessio (1996), D’Alessio et al. (1998, 1999), D’Alessio, Calvet & Hartmann (2001) and Calvet et al. (2002). They have compared observations of CTTS to self-consistent physical models of disks around young low mass stars. These models include the effect of both, stellar irradiation and viscous dissipation, allowing to cover the parameter space from “passive” to “active” disks. They also consider opacities of bigger dust grains than those characteristic of the Interstellar Medium (ISM), in a preliminary attempt to study dust evolution in disks around CTTS.

2. DETAILED PHYSICAL MODELS OF DISKS

D’Alessio et al. (1996; 1998; 1999; 2001) have developed a method to calculate the structure and emergent intensity of α -accretion disks irradiated by their central star. Details about the assumptions and equations can be found in those papers and here we only mention the main assumptions. The disk structure is calculated given its central star properties (mass, radius and effective temperature) and the disk mass accretion rate \dot{M} , viscosity parameter α and dust properties. The transfer of stellar radiation through the disk is calculated taking into account its shorter wavelength and impinging direction, and assuming a plane-parallel geometry. We use the first two moments of the radiative transfer equation and the Eddington approximation. The degree of *flaring* of the disk surface, which affects the

fraction of stellar radiation intercepted and how it is deposited in the disk atmosphere, is calculated self-consistently. We assume the energy is transported by radiation, convection and a turbulent energy flux consistent with the α -prescription. The disk main heating mechanisms are viscous dissipation and stellar irradiation. For completeness, we include the heating by ionization produced by cosmic rays and radioactive decay of ^{26}Al , that might become important in non-irradiated cases (D’Alessio 1996).

The opacity is a crucial ingredient in the calculation of the disk thermal structure, and given the range of typical temperatures, the dust is the most important opacity source. Different kinds of mean opacities are used to describe the interaction between the dust and the stellar/disk radiation fields. Given the structure and a particular inclination angle between the disk axis and the line of sight, the radiative transfer equation is integrated using monochromatic opacities. Mean and monochromatic dust opacities are calculated self-consistently for given abundances, distribution of grain sizes, optical properties, etc. Finally, the monochromatic emergent intensity is used to construct both, the disk SED and its images, considering different spatial resolutions.

3. DUST EVOLUTION

Theories of dust evolution in disks predict settling and runaway growth of grains in timescales of $\sim 10^4$ years (Weidenschilling 1988; Weidenschilling & Cuzzi 1993). In principle, observations and detailed modeling of T Tauri disks might help to test and constrain dust evolution theories.

From observations in the mm spectral range it is clear that the dust in disks is different from the dust in the ISM (Beckwith & Sargent 1991, hereafter BS91; Mannings & Emerson 1994). BS91 analyze the spectral index $n = d \log F_\nu / d \log \nu$ in mm wavelengths of an important fraction of CTTS, finding that it is much smaller than what would be expected for ISM dust in an optically thin disk. If the mm opacity is approximated by a power law $\kappa_\nu \sim \nu^\beta$, an optically thin disk should have $n = \beta + 2$. ISM dust has $\beta = 2$ (e.g. Draine & Lee 1984), but SEDs of CTTS typically show $n = 2 - 3$, corresponding to $\beta = 0 - 1$. BS91 propose that the dust grains in disks are bigger than in the ISM (see review by Beckwith, Henning & Nakagawa 2000).

3.1. Disks with ISM dust

D’Alessio et al. (1999) calculate self-consistent models of irradiated accretion disks with ISM dust. They assume that dust and gas are well mixed and

thermally coupled. Dust optical properties were taken from Draine & Lee (1984), and the adopted size distribution was the standard MRN (Mathis, Rumpl, Nordsieck 1977), $n(a) \sim a^{-3.5}$ where a is the grain radius. The minimum and maximum sizes were $a_{min} = 0.005 \mu m$ and $a_{max} = 0.25 \mu m$. The main conclusion of that work is that these ISM-dust disks were more geometrically thick than observed disks, based on the following results:

- The models show a larger far-IR excess than observed in typical SEDs of CTTS. The disk “irradiation” surface, where the optical depth to the stellar radiation is one, determines the fraction of intercepted stellar radiative flux. Since the emergent far-IR flux is reprocessed stellar flux, the predicted large excess is a consequence of a high irradiation surface. As we already mentioned, the height and shape of the irradiation surface (degree of flaring) is a result of the models, such that the larger the dust opacity around $\sim 1 \mu m$, the higher the irradiation surface.
- The models also show wider dark lanes than in observed scattered light near-IR images of edge-on disks. The thickness of the dark lane in these images depends mostly on the dust opacity to the stellar radiation, i.e, around $\sim 1 \mu m$.
- We predict a larger number of stars occulted by their disks (“edge-on” disks) than consistent with current surveys. Assuming random orientations respect to the line of sight, the fraction of disks with an inclination larger than i is given by $\cos i$. We find that between 30 and 40 % of the star+disk systems should have an extinction $A_V > 30$ mag. However, observations suggests that less than 15 % of the systems have these high extinctions. Again, models are too geometrically thick.
- In spite of the fact that the models do not include the assumption that the disks are optically thin, they exhibit too little mm and submm emission compared to observations (e.g. BS91), and that $n \sim 2$.

These deficiencies are a consequence of problems in the adopted dust opacity at short wavelengths ($\sim 1 \mu m$) and emissivity at long wavelengths ($\sim mm$). Thus, the dust in disks is different from the dust in the ISM and, probably, dust and gas are not well mixed. D’Alessio et al.(1999) propose that the problems of the models can be relieved or eliminated by including grain growth and settling to the disk

midplane. Both processes are explored in a parameterized approach trying to use few parameters.

3.2. Disks with Grain Growth

When the sizes of the grains increases but the mass in dust remains constant, the fraction of grains in each size interval changes. The opacity at a given wavelength is dominated by grains with a size similar to the wavelength, thus a change in the distribution of sizes affects the dust opacity at every wavelength. Figure 1 shows the dust total opacity and the absorption coefficient at two representative wavelengths $\lambda = 0.8 \mu m$ and $1.3 mm$, for a distribution of grain sizes $n(a) \sim a^{-p}$, with $p = 3.5$, as a function of maximum grain size, a_{max} . At both wavelengths, it can be seen that the opacity is larger for a_{max} of the order of the wavelength (see also Miyake & Nakagawa 1993). Let us consider the opacity at $0.8 \mu m$ as representative of how the disk absorbs the stellar radiation. Thus, the bigger the a_{max} , the smaller this opacity, and the deeper the stellar radiation can penetrate the disk. On the other hand, the opacity (and the emissivity) at $1.3 mm$ increases for $a_{max} \sim 1 mm$. Figure 1 also shows that the absorption coefficient proposed by BS91,

$$\kappa_\nu = 0.1 \left(\frac{\lambda}{250 \mu m} \right)^{-1},$$

represents an upper limit for the opacity at $1.3 mm$, only valid for $a_{max} \sim 1 mm$. If the maximum grain size is different from $1 mm$ then disk masses, inferred using this coefficient and the observed mm fluxes, are underestimated.

The way in which the opacity changes with wavelength when a_{max} increases, suggests that disk models with **bigger** dust grains should compare better with observations than disks with ISM dust. Thus, D’Alessio, Calvet & Hartmann (2001) construct *well mixed* disk models with different values of a_{max} and the exponent p . They find that:

- The irradiation surface of the disk and its IR excess decrease with a_{max} .
- The median SED of CTTS in the Taurus molecular cloud, from near-IR to mm wavelengths, can be fitted by a model with $a_{max} \approx 1 mm$.
- The width of the dark lane in scattered light images of edge-on disks decreases with a_{max} and increases with p . A model with typical disk parameters and $a_{max} \sim 1 mm$ can explain the observed width in the case of HH 30 and HK Tau B (see their figures 8 and 9).

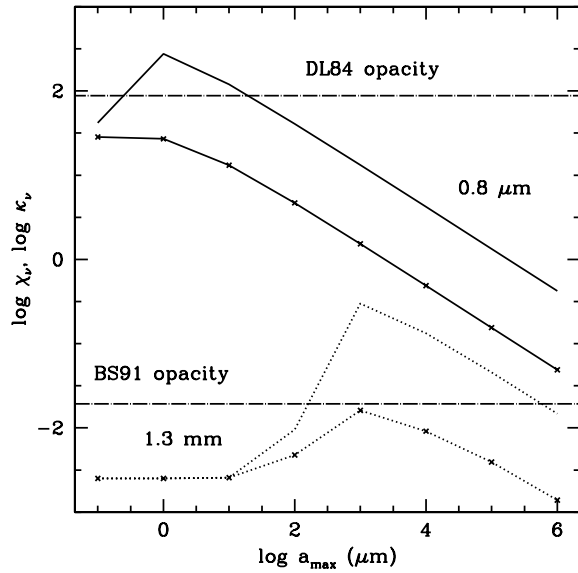


Fig. 1. Dust opacity at $\lambda = 0.8 \mu\text{m}$ (solid lines) and 1.3 mm (dotted lines), for a distribution of sizes $n \sim a^{-3.5}$, with $a_{\text{min}} = 0.005 \mu\text{m}$ and different a_{max} . The curves with dots correspond to the true absorption coefficient only, κ_ν , and the curves without dots include the scattering coefficient, $\chi_\nu = \kappa_\nu + \sigma_\nu$. The horizontal lines represent the opacity for ISM dust at $0.8 \mu\text{m}$ (labelled DL84 after Draine & Lee 1984) and the opacity proposed by BS91 at 1.3 mm (labelled BS91)

- The fraction of occulted central stars is 20 % for $a_{\text{max}} = 1 \text{ mm}$ and 10 % for $a_{\text{max}} = 10 \text{ cm}$, i.e., more consistent with current surveys.

3.3. Quantifying disks properties

There is an unfortunate degeneracy between the disk mass and the dust opacity. When the dust opacity is related to the grain size distribution, it seems impossible to distinguish a low mass disk with small grains from a high mass disk with big grains by means of a near-IR scatter light image. An example of this is the case of HK Tau B. This object is observed by Stapelfeldt et al. (1998) using *HST* at $\sim 0.8 \mu\text{m}$, and they find a disk model with a mass $M_d = 10^{-4} M_\odot$ and **ISM dust** that fits the observed image. On the other hand, D'Alessio et al. (2001) propose that a disk model with almost 1000 times more mass and typical stellar and disk parameters, but bigger grains with $a_{\text{max}} = 1 \text{ m}$ and $p = 3.5$, can also explain the observed image. Another example is LkH α 262 in MBM12 (Jayawardhana et al. 2002). The observed images in the J, H and K bands can be explained by different disk models with values of the disk mass and maximum

grain radius $(M_d, a_{\text{max}}) = (2 \times 10^{-4} M_\odot, 10 \mu\text{m})$ or $(2 \times 10^{-3} M_\odot, 1 \text{ mm})$ or $(2 \times 10^{-2} M_\odot, 10 \text{ cm})$.

In the mm range, grain growth affects both the predicted flux and the spectral index. Figure 2 shows a sequence of irradiated *well mixed* disk models with masses $M_d = 0.02$ (dashed line), 0.05 (solid line) and 0.09 (dot-dashed line) M_\odot and different values of a_{max} from $10 \mu\text{m}$ (at the right end of the curves) to 10 cm (at the left end). The triangles are models with the same masses, but ISM dust. The circled dots on the curves corresponds to *well mixed* disk models with $a_{\text{max}} = 1 \text{ mm}$. The circled dots at the left bottom of the panels corresponds to models of *flat* disks, also with $a_{\text{max}} = 1 \text{ mm}$, which represents an extreme case of dust settling. When compared to observations of CTTS in Taurus (stars), the *well mixed* models can account for those objects with $n \gtrsim 2$. For the cases with smaller values of n , we propose two alternatives: (i) the dust in the disk is settling towards the midplane, thus an intermediate model between a *well mixed* and a *flat* disk could explain the observed fluxes, and (ii) the disk has a large mass accretion rate and its outer regions are not irradiated by the central star (in a shadow; e.g. Bell et al. 1997). For the well mixed models, we can see that the flux depends on both a_{max} and M_d , and there is a degeneracy between the two variables for $a_{\text{max}} > \lambda$. However, the spectral index n depends on a_{max} for $a_{\text{max}} > \lambda$. This means that observations at $\lambda \sim a_{\text{max}}$ show variations that could help to disentangle M_d and a_{max} .

Another example of such effect is the disk 114-426 in Orion, that shows grey opacity between 0.7 and $1.9 \mu\text{m}$, suggesting $a_{\text{max}} > 5 \mu\text{m}$ (Throop et al. 2001). Also, the width of the dark lane vs λ in the scattered light image of an edge-on disk can be related to the scattering asymmetry factor g , which in turn depends on a_{max} . The observations of HH 30 suggest that a_{max} is ~ 2 times the maximum size of ISM grains (Cotera et al. 2001).

It is important to mention that the observations we have discussed here can be used to characterize grain growth in the atmosphere and/or outer regions of the disk. As we already discussed, the IR continuum is sensitive to the atmospheric opacity to the stellar radiation. The near-IR bands are formed in the hot upper atmosphere and their emissivity depends on the atmospheric dust content. On the other hand, in radio-frequencies radiation escapes from regions closer to the midplane. Since the disk area increases with distance to the star, the total emergent flux is dominated by the outer disk. Thus, mm fluxes and spectral indices are proving grain growth at the

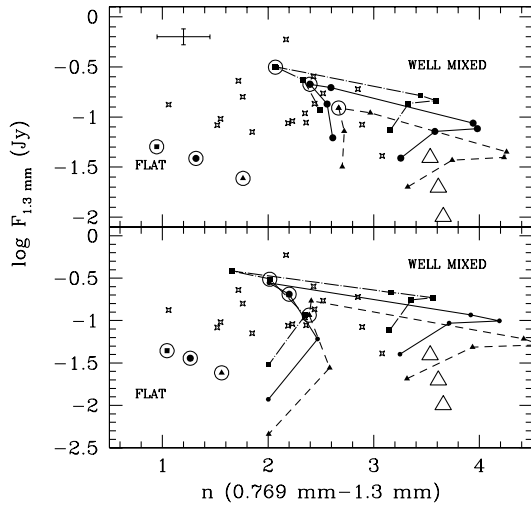


Fig. 2. Model disk flux at 1.3 mm vs spectral index between 0.769 mm and 1.3 mm compared with observed values (stars) from BS91. Upper panel: for $n \sim a^{-3.5}$. Lower panel: for $n \sim a^{-2.5}$. In both cases, $a_{max} = 10, 100, 120, 150, 300 \mu\text{m}, 1 \text{ mm}, 1 \text{ cm}, \text{ and } 10 \text{ cm}$. See text for details.

midplane of the outer disk. Also scattered light images of edge-on disks are sensitive to the properties of the dust, both at the disk atmosphere and in the outer disk. The dust in the atmosphere is responsible for scattering the stellar light, that has to be transmitted through the outer regions. In our well mixed disk models we assume that the dust content is the same everywhere in the disk, but this is just a simplifying assumption.

3.4. Dust growth in the inner disk

It is expected that grains grow and, eventually, form planets, and a giant planet inside a disk opens a gap (Lin & Papaloizou 1986; 1993; Bryden et al. 1999). We find evidences of a gap developing in the inner disk of TW Hya, a 10 Myrs old CTTS, still accreting mass from its disk ($\dot{M} = 5 \times 10^{-10} M_{\odot} \text{ yr}^{-1}$ - Muzerolle et al. 2000; $\sim 10^{-8} M_{\odot} \text{ yr}^{-1}$ - Alencar & Batalha 2001). Its SED shows almost no-excess above the stellar photosphere for $\lambda < 8 \mu\text{m}$, a strong $10 \mu\text{m}$ silicate band in emission and a large excess around $20 \mu\text{m}$. Based on the SED, we propose a model for this object in which the disk has a gap at $R < 4 \text{ AU}$, with a some remnant small dust grains and gas. Between the gap and the outer disk, there is a bright rim that receives stellar radiation frontally (Calvet et al. 2001). This rim is similar to the one

proposed by Natta et al. (1999) and Dullemond et al. (2000) to explain the $3 \mu\text{m}$ excess in Ae stars. However, in the case of TW Hya, the rim should be located at a distance larger than the dust condensation radius to explain the observed excess at $20 \mu\text{m}$. We propose that the rim is at the outer radius of a gap, produced by a growing body in the inner disk. Unfortunately, the gap cannot be resolved by the VLA at 7 mm, thus observations at higher spatial resolution are required to further test this model.

3.5. Disks with dust Settling

The median SED of CTTS in Taurus is consistent with a disk model with typical parameters, i.e., $\dot{M} = 10^{-8} M_{\odot} \text{ yr}^{-1}$, $\alpha = 0.01$, $M_{*} = 0.5 M_{\odot}$, $R_{*} = 2 R_{\odot}$, $T_{*} = 4000 \text{ K}$, $R_d = 100 \text{ AU}$, in which grains are allowed to grow up to $a_{max} \sim 1 \text{ mm}$. However, there is an important property that cannot be explained by this model: the $10 \mu\text{m}$ silicate band in emission (Natta, Meyer & Beckwith 2000). If the band is produced in the upper hot atmosphere of irradiated disks then the atmospheric grains should have $a_{max} \lesssim 1 \mu\text{m}$. The emission of bigger grains tend to wash-out the feature. But such a small value of a_{max} for a **standard dust to gas mass ratio**, makes the disk too thick, and it has the same problems as the disk with ISM dust described in §3.1. Thus, the model that explains the median SED cannot explain the $10 \mu\text{m}$ silicate band, unless the assumption of well mixed dust and gas is relaxed. If the larger grains fall towards the midplane, the disk atmosphere is free from big grains but also it has a **lower dust to gas mass ratio than the standard value**. This implies a lower opacity at every wavelength, but in particular at short-wavelength. Thus, a disk model with settling can have the same continuum SED as the model with large a_{max} (e.g., Miyake & Nakagawa 1995) but also an important $10 \mu\text{m}$ emission band. This composite model is illustrated in Fig. 3, by the SED of a disk in which the atmospheric dust grains have grown to $a_{max} \sim 300 \mu\text{m}$, but all the grains with $a > 1 \mu\text{m}$ have settled. In this case, the dust to gas mass ratio in the atmosphere is 5×10^{-4} , instead of the standard value 10^{-2} .

Chiang et al. (2001) also have calculated two-layer disk models with different values of a_{max} in the atmosphere and in the interior. In these models, the ‘‘irradiation surface’’ is introduced as an additional input parameter (or function), and not as the result of the properties of dust in the atmosphere. However, they find several objects that only can be fitted by small atmospheric grains and a flat disk surface, which would be consistent with the inter-

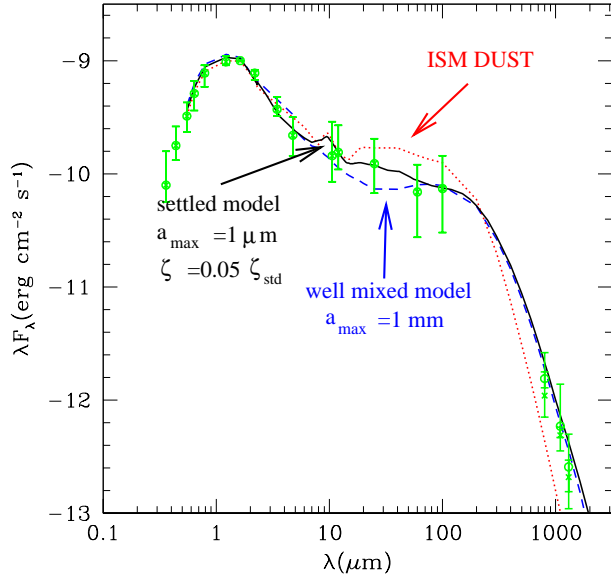


Fig. 3. SED of disk models with standard values of \dot{M} , α , central star properties and different assumptions for the dust: well mixed ISM dust (dotted line), well mixed grains with $a_{max} = 1$ mm (dashed line) and dust settling, with an atmospheric value of $a_{max} = 1 \mu\text{m}$ and a mid-plane value of 1 mm (solid line). The points represent the median observed SED of CTTS in Taurus (D'Alessio et al. 1999).

pretation of dust growing and settling in the disk atmosphere.

4. CONCLUSIONS

Detailed physical models of accretion disks irradiated by the central star, compared to observations, can be used to quantify physical properties of disks such as their masses and grain sizes. However, it is important to cover a wide range of wavelengths, since only when $\lambda \sim a_{max}$ it seems possible to disentangle disk masses from maximum grain sizes.

In particular, the median SED of CTTS in Taurus can be explained by both, a *well mixed* disk model with $a_{max} = 1$ mm or a *settled* model with $a_{max}^{atm} = 1 \mu\text{m}$, but in which a large fraction of the atmospheric dust has settled towards the midplane. In the first case, the model predicts no silicate $10 \mu\text{m}$ band, and in the second case the model predicts a strong band. In principle, by combining information from the continuum and the band, one can attempt to quantify the degree of settling.

It is important to construct models in which the properties of dust change spatially, as a result of dust evolution (e.g. growing, settling). These models should incorporate dust properties self-consistently into the calculation of the disk structure, since with-

out physical constraints, one can get lost in the parameter space.

I want to thank M. Peña for her invitation. J. Ballesteros for careful reading of the manuscript and useful comments. I acknowledge financial support from DGAPA-UNAM and CONACYT-México. This work has made extensive use of NASA's Astrophysics Data System Abstract Service.

REFERENCES

- Alencar, S. H. P. & Batalha, C. 2002, ApJ, 571, 378
 Alencar, S. H. P., Johns-Krull, C. M., & Basri, G. 2001, AJ, 122, 3335
 Ardila, D. R. & Basri, G. 2000, ApJ, 539, 834
 Balbus, S. A. & Hawley, J. F. 1991, ApJ, 376, 214
 Beckwith, S.V.W., & Sargent, A.I. 1991 ApJ, 381, 250 (BS91)
 Beckwith, S. V. W., Henning, T. & Nakagawa, Y., 2000, in Protostars and Planets IV, (Tucson: University of Arizona Press), eds Mannings, V., Boss, A.P., Russell, S. S, p. 533
 Bell, K. R. & Lin, D. N. C. 1994, ApJ, 427, 987
 Bell, K. R., Cassen, P. M., Klahr, H. H., & Henning, T. 1997, ApJ, 486, 372
 Bertout, C., Basri, G., & Bouvier, J. 1988, ApJ, 330, 350
 Bryden, G., Chen, X., Lin, D. N. C., Nelson, R. P., & Papaloizou, J. C. B. 1999, ApJ, 514, 344
 Calvet, N., Patiño, A., Magris, G., & D'Alessio, P. 1991, ApJ, 380, 617 (CPMD).
 Calvet, N., Magris, G., Patiño, A., & D'Alessio, P. 1992, Rev. Mex. Astronom. Astrofís., 24, 27
 Calvet, N. and Gullbring, E. 1998, ApJ, 509, 802
 Calvet, N., D'Alessio, P., Hartmann, L., Wilner, D., Walsh, A., & Sitko, M. 2002, ApJ, 568, 1008
 Chiang, E.I., & Goldreich, P., 1997 ApJ, 490, 368 (CG)
 Chiang, E. I., Joungh, M. K., Creech-Eakman, M. J., Qi, C., Kessler, J. E., Blake, G. A., & van Dishoeck, E. F. 2001, ApJ, 547, 1077
 Cotera, A. S. et al. 2001, ApJ, 556, 958
 D'Alessio, P. 1996, Ph.D. Thesis, Universidad Nacional Autónoma de México, México
 D'Alessio, P., Cantó, J., Calvet, N., & Lizano, S. 1998, ApJ, 500, 411 (DCCL) (Paper I)
 D'Alessio, P., Calvet, N., Hartmann, L., Lizano, S. and Cantó, J. 1999, ApJ, 527, 893 (Paper II)
 D'Alessio, P., Calvet, N., & Hartmann, L. 2001, ApJ, 553, 321 (DCH01)
 Draine, B. T., & Lee, H. M. 1984, ApJ, 285,89
 Dullemond, C. P., Dominik, C., & Natta, A. 2001, ApJ, 560, 957
 Dutrey, A., Guilloteau, S., Duvert, G., Prato, L., Simon, M., Schuster, K., & Menard, F. 1996, A&A, 309, 493
 Gullbring, E., Hartmann, L., Briceño, C., & Calvet, N. 1998, ApJ, 492, 323
 Gullbring, E., Calvet, N., Muzerolle, J., & Hartmann, L. 2000, ApJ, 544, 927

- Hartmann, L., Hewett, R., & Calvet, N. 1994, *ApJ*, 426, 669
- Hartmann, L. 1998, *Accretion processes in star formation / Lee Hartmann*. Cambridge, UK ; New York : Cambridge University Press, 1998. (Cambridge astrophysics series ; 32) ISBN 0521435072.,
- Hartmann, L., Calvet, N., Gullbring, E., & D'Alessio, P. 1998, *ApJ*, 495, 385
- Jayawardhana, R., Luhman, K. L., D'Alessio, P., & Stauffer, J. R. 2002, *ApJ*, 571, L51
- Johns-Krull, C. M., Valenti, J. A., & Koresko, C. 1999, *ApJ*, 516, 900
- Johns-Krull, C. M. & Valenti, J. A. 2001, *ApJ*, 561, 1060
- Kenyon, S.J., & Hartmann, L. 1987, *ApJ*, 323, 714 (KH87)
- Koresko, C. D. 1998, *ApJ*, 507, L145
- Krist, J. E., Stapelfeldt, K. R., Ménard, F., Padgett, D. L., & Burrows, C. J. 2000, *ApJ*, 538, 793
- Lin, D. N. C., & Papaloizou, J. 1986, *ApJ*, 309, 846
- Lin, D. N. C., & Papaloizou, J. 1993, in *Protostars and Planets III*, ed. E. H. Levy & J. L. Lunine (Tucson: Univ. Arizona Press), 749
- Lynden-Bell, D. & Pringle, J. E. 1974, *MNRAS*, 168, 603
- Mannings, V. & Emerson, J. P. 1994, *MNRAS*, 267, 361
- Mathis, J. S., Rumpl, W., & Nordsieck, K. H. 1977, *ApJ*, 217, 425
- McCaughrean, M. J., Stapelfeldt, K. R., & Close, L. M. 2000, *Protostars and Planets IV*, 485
- Miyake, K., & Nakagawa, Y. 1993, *Icarus*, 106, 20 (MN93)
- Miyake, K., & Nakagawa, Y. 1995, *ApJ*, 441, 361
- Muzerolle, J., Calvet, N., & Hartmann, L. 1998, *ApJ*, 492, 743
- Muzerolle, J., Hartmann, L., & Calvet, N. 1998, *AJ*, 116, 455
- Muzerolle, J., Calvet, N., Briceño, C., Hartmann, L., & Hillenbrand, L. 2000, *ApJ*, 535, L47
- Muzerolle, J., Calvet, N., & Hartmann, L. 2001, *ApJ*, 550, 944
- Natta, A., Prusti, T., Neri, R., Thi, W. F., Grinin, V. P., & Mannings, V. 1999, *A&A*, 350, 541
- Natta, A., Meyer, M.R., Beckwith, S.V.W. 2000, *ApJ*, 534, 8
- Pollack, J. B., Hollenbach, D., Beckwith, S., Simonelli, D. P., Roush, T. & Fong, W. 1994, *ApJ*, 421, 615 (P94)
- Shakura, N. I. & Sunyaev, R. A. 1973, *A&A*, 24, 337
- Shu, F. H., Adams, F. C., & Lizano, S. 1987, *ARA&A*, 25, 23
- Stapelfeldt, K.R., Krist, J.E., Ménard, F., Bouvier, J., Padgett, D.L., & Burrows, C.J. 1998, *ApJ*, 502, L65
- Stone, J. M., Gammie, C. F., Balbus, S. A., & Hawley, J. F. 2000, *Protostars and Planets IV*, 589
- Weidenschilling, S.J. & Cuzzi, J.N. 1993, in *Protostars and Planets III*, eds. E.H. Levy & J.I. Lunine (Tucson: University of Arizona Press), p. 1031
- Weidenschilling, S.J. 1997, *Icarus*, 127, 290
- Wilner, D. J. & Lay, O. P. 2000, *Protostars and Planets IV*, 509